J|A|C|S
ARTICLES
Published on Web 09/09/2006

Synthesis and Characterization of Iron Silicon Boron (Fe_5Si_2B) and Iron Boride (Fe_3B) Nanowires

Yan Li and R. P. H. Chang*

Contribution from the Department of Materials Science and Engineering, and Materials Research Institute, Northwestern University, 2220 Campus Drive, Evanston, Illinois 60208-3108

Received February 13, 2006; E-mail: r-chang@northwestern.edu

Abstract: Single-crystal iron silicon boron (Fe_5Si_2B) and iron boride (Fe_3B) nanowires were synthesized by a chemical vapor deposition (CVD) method on either silicon dioxide (SiO_2) on silicon (Si) or Si substrates without introducing any catalysts. FeI_2 and BI_3 were used as precursors. The typical size of the nanowires is about 5−50 nm in width and 1−20 μm in length. Different kinds of Fe−Si−B and Fe−B structures were synthesized by adjusting the ratio of FeI_2 vapor to BI_3 vapor. Single-crystal Fe_5Si_2B nanowires formed when the FeI_2 sublimator temperature was kept in the range of 540−570 °C. If the FeI_2 sublimator temperature was adjusted in the range of 430−470 °C, single-crystal Fe_3B nanowires were produced. Fe_3B nanowires grow from polycrystalline Fe_5SiB_2 particles, while Fe_5Si_2B nanowires grow out of the Fe_5Si_2B layers, which are attached to triangle shaped FeSi particles. Both the ratio of FeI_2 vapor to BI_3 vapor and the formation of the particles (Fe_5SiB_2 particles for the growth of Fe_3B nanowires, FeSi particles for the growth of Fe_5Si_2B nanowires) are critical for the growth of Fe_3B and Fe_5Si_2B nanowires. The correct FeI_2 vapor to BI_3 vapor ratio assures the desired phase form, while the particles provide preferential sites for adsorption and nucleation of Fe_3B or Fe_5Si_2B molecules. Fe_3B or Fe_5Si_2B nanowires grow due to the preferred growth direction of <110>.

Introduction

Both Fe−Si−B- and Fe−B-based alloys are promising structural and magnetic materials with excellent mechanical properties as well as unique soft magnetic properties.[1−11] For example (Fe, Co)−B−Si−Nb glassy alloys exhibit superhigh fracture strength of 3900−4250 MPa, Young's modulus of 190−210 GPa, elastic strain of 0.02, and plastic strain of 0.0025. They also show good soft magnetic properties with saturation magnetization of 0.84−1.13 T, low coercive force of 1.5−2.7 A/m, high permeability exceeding 1.2×10^4, and Curie temperature of 600−690 K[1]. Magnetic property studies of tetragonal Fe_3B flakes made by isothermal annealing of amorphous $Fe_{76}B_{24}$ flakes show that tetragonal Fe_3B is a soft magnetic metal with a saturation magnetization of 1.6 T, a coercive field, $\mu_0 H_c$, around 0.3 T, a curie temperature of 786 K, and a domain wall thickness of 20 nm.[8,9] The hardness and the reduced Young's modulus of amorphous iron boride films deposited on glass substrates are measured to be 20 and 200 Gpa, respectively.[5] It has been found that crystallization of Fe−Si−B-based alloys can improve their magnetic properties.[12] The crystallization kinetics of Fe−Si−B metallic glasses at different chemical composition has been studied using a variety of techniques.[13−16] We have reported the synthesis of Fe_3B nanowires on sapphire substrates by a chemical vapor deposition (CVD) method, which employs BI_3 and FeI_3 as precursors and Pt/Pd films as catalysts.[17] Here we report the synthesis and characterization of both Fe_5Si_2B and Fe_3B nanowires on Si or SiO_2 on Si substrates without introducing any catalysts. Both Fe_5Si_2B nanowires and Fe_3B nanowires can have excellent mechanical properties as well as superior magnetic properties. They may have potential for use as MFM tips and magnetic data storage media.[17] They can also be building blocks in magnetic sensors, magnetic recording heads, magnetic memories, and magnetic composites.[17−24]

(1) Shen, B.; Inoue, A.; Chang, C. *Appl. Phys. Lett.* **2004**, *85*, 4911.
(2) Amiya, K.; Urata, A.; Nishiyama, N.; Inoue, A. *Mater. Trans.* **2004**, *45*, 1214.
(3) Inoue, A.; Shen, B.; Yavari, A. R.; Greer, A. L. *J. Mater. Res.* **2003**, *18*, 1487.
(4) Inoue, A.; Katsuya, A.; Amiya, K.; Masumoto, T. *Mater. Trans.* **1995**, *36*, 802.
(5) Dehlinger, A. S.; Pierson, J. F.; Roman, A.; Bauer, P. *Surf. Coat. Technol.* **2003**, *174*, 331.
(6) Sen, S.; Ozbek, I.; Sen, U.; Bindal, C. *Surf. Coat. Technol.* **2001**, *135*, 173.
(7) Dorofeev, V. Y.; Selevtsova, I. V. *Powder Metall. Metal Ceram.* **2001**, *40*, 452.
(8) Coehoorn, R.; Demooij, D. B.; Dewaard, C. *J. Magn. Magn. Mater.* **1989**, *80*, 101.
(9) Coene, W.; Hakkens, F.; Coehoorn, R.; Demooij, D. B.; Dewaard, C.; Fidler, J.; Grossinger, R. *J. Magn. Magn. Mater.* **1991**, *96*, 189.
(10) Kong, Y.; Li, F. S. *Phys. Rev. B* **1997**, *56*, 3153.
(11) Chien, C. L.; Musser, D.; Gyorgy, E. M.; Sherwood, R. C.; Chen, H. S.; Luborsky, F. E.; Walter, J. L. *Phys. Rev. B* **1979**, *20*, 283.
(12) Yoshizawa, Y.; Oguma, S.; Yamauchi, K. *J. Appl. Phys.* **1988**, *64*, 6044.
(13) Gibson, M. A.; Delamore, G. W. *J. Mater. Sci.* **1992**, *27*, 3533.
(14) Ramanan, V. R. V.; Fish, G. E. *J. Appl. Phys.* **1982**, *53*, 2273.
(15) Kunitomi, N. *Mater. Sci. Eng.* **1994**, *A179/A180*, 293.
(16) Susic, M.; Maricic, A. M. *Mater. Chem. Phys.* **1992**, *30*, 221.
(17) Li, Y.; Tevaarwerk, E.; Hsieh, K.; Chang, R. P. H. *Chem. Mater.* **2006**, *18*, 2552.
(18) Dennis, C. L.; Borges, R. P.; Buda, L. D.; Ebels, U.; Gregg, J. F.; Hehn, M.; Jouguelet, E.; Ounadjela, K.; Petej, I.; Prejbeanu, I. L.; Thorntorn, M. J. J. *J. Phys.: Condens. Matter.* **2002**, *14*, R1175.
(19) Henry, Y.; Ounadjela, K.; Piraux, L.; Dubois, S.; George, J.-M.; Duvail, J.-L. *Eur. Phys. J. B* **2001**, *20*, 35.
(20) Garcia, J. M.; Thiaville, A.; Miltat, J. *J. Magn. Magn. Mater.* **2002**, *249*, 163.

10.1021/ja0610378 CCC: $33.50

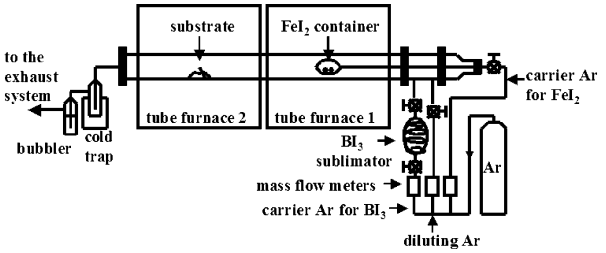

Figure 1. Schematic of the CVD apparatus.

Experimental Procedure

The CVD apparatus shown in Figure 1 is similar to the one used to grow Fe_3B nanowires on Pt/Pd-coated sapphire substrates.[17] The whole system, including the gas tubing after three mass flow meters, the valves, the chamber, the cold trap, and the bubbler, is all made of quartz or glass to avoid metal contamination. Different quartz reactor with the same size was used to eliminate metal catalysts introduced during previous runs. After each run, the quartz reactor was cleaned with 5% hydrofluoric acid (HF) to eliminate contaminations from the previous run. Tube furnace 1 was used to heat the FeI_2 container, while tube furnace 2 controlled the temperature of the substrates. A Si or SiO_2 on Si substrate was placed on a quartz boat, which was then pushed to the center of tube furnace 2. Tube furnace 1 and tube furnace 2 were heated to 420−600 and 800 °C, respectively, under Ar flow. Once the desired temperatures of the two furnaces were reached, the FeI_2 container was pushed to the center of tube furnace 1. There is a small hole on one side of the FeI_2 sublimator and an opening on the other side that is connected to a feed through quartz tubing. The two valves at both ends of the BI_3 sublimator were then opened. The temperature of the BI_3 sublimator was controllable and usually kept at 31 °C. The FeI_2 (99.99+%, Aldrich) and BI_3 (98+%, Aldrich) powder[25] were transferred into their sublimators inside a glove box to prevent them from reacting with H_2O vapor and O_2 in air. Ar gas was introduced as a carrier gas for both FeI_2 and BI_3 and also served as a diluting gas. The typical flow rates were 10−20, 10, and 200 sccm, respectively. The reaction time was varied from 5 min to 2 h. After reaction, the FeI_2 container was pulled back to the inlet of the reactor, the valves of the BI_3 sublimator were closed, and the two tube furnaces were cooled down to room temperature under Ar gas flow.

A scanning electron microscope (Hitachi S-4500 FE-SEM) was used to observe the morphology of the structures formed on the substrates. X-ray diffraction (XRD, Rigaku DMAX-A diffractometer with Ni filter, 1.54184 Å Cu Kα radiation), a transmission electron microscope (TEM, Hitachi H8100 and Hitachi HF2000), and selected area electron diffraction (SAED, Hitachi H8100) were employed to characterize the crystal structures. The TEM specimens were made by dragging holey carbon grids (400 mesh Cu, SPI supplies) along the surface of the samples. Chemical composition of the structures was studied by electron energy-loss spectrometry (EELS, Hitachi HF2000 with a Gatan Imaging Filter (GIF) system, JEOL JEM-2100F with GIF system) and X-ray energy-dispersive spectrometry (XEDS, Hitachi HF2000 with a UTW X-ray detector, JEOL JEM-2100F with a UTW X-ray detector).

Results and Discussions

Synthesis and Characterization of Fe_3B Nanowires. Various kinds of products form by adjusting the temperature of the FeI_2 sublimator, as illustrated in Table 1. The vapor pressures of both FeI_2 and BI_3 are controlled by the temperature of the sublimator. The amount of FeI_2 and BI_3 vapor introduced in the chamber is determined by both the temperature of each sublimator and the flow rate of each carrier gas. Modifying the temperature of the FeI_2 sublimator while keeping all the other growth conditions unchanged is actually changing the ratio of FeI_2 vapor to BI_3 vapor introduced to the reaction zone of the CVD system. Figure 2 shows typical SEM images of the structures formed when the FeI_2 sublimator temperature was kept in the range of 430−470 °C. It reveals that many nanowires grow out of microscale particles around the scratches deliberately drawn by a diamond-tipped scriber of SiO_2 on Si substrates, where the SiO_2 layer was removed. The SiO_2 layer serves as a mask for the growth of nanowires. If a Si substrate

Table 1. Products Formed on SiO_2 on Si or Si Substrates when the FeI_2 Sublimator Temperature is Modified from 420 to 600 °C[a]

FeI_2 sublimator temperature	products
<430 °C	nothing formed
430−470 °C	Fe_5SiB_2 particles with Fe_3B nanowires
480−530 °C	Fe_3Si_3B particles, $FeSi_2$ particles
540−570 °C	FeSi particles with Fe_5Si_2B nanowires, $FeSi_2$ particles
>585 °C	large FeSi particles

[a] Growth conditions: substrate temperature = 800 °C, diluting Ar flow = 200 sccm, carrier Ar with FeI_2 (FeI_2 sublimator temperature = 420 − 600 °C) flow = 10−20 sccm, carrier Ar with BI_3 (BI_3 sublimator temperature = 31 °C) flow = 10 sccm, growth time: 0.5−2 h.

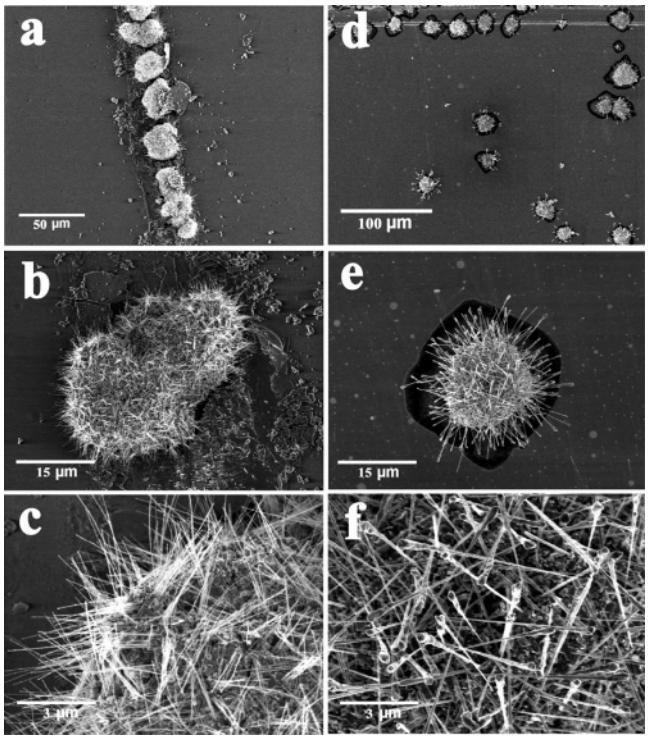

Figure 2. (a−c) SEM images of the nanowires synthesized on a bare SiO_2 on Si substrate at 800 °C with 10 sccm Ar gas carried FeI_2 vapor (FeI_2 sublimator temperature = 430 °C), 10 sccm Ar gas carried BI_3 vapor (BI_3 sublimator temperature = 31 °C), and 200 sccm diluting Ar gas flowing for 1 h. (d−f). SEM images of the nanowires synthesized on a Si substrate after heating at 800 °C under 15 sccm Ar gas carried FeI_2 vapor (FeI_2 sublimator temperature = 445 °C), 10 sccm Ar gas carried BI_3 vapor (BI_3 sublimator temperature = 31 °C), and 200 sccm diluting Ar gas flow for 2 h.

(21) Spaldin, N. A. *Magnetic Materials: Fundamentals and Device Applications*; Cambridge Universty Press: New York, 2003.
(22) Wegrowe, J.-E.; Kelly, D.; Franck, A.; Gilbert, S. E.; Ansermet, J.-P. *Phys. Rev. Lett.* **1999**, *82*, 3681.
(23) Dubois, S.; Marchal, C.; Beuken, J. M.; Piraux, L.; Duvail, J. L.; Fert, A.; George, J. M.; Maurice, J. L. *Appl. Phys. Lett.* **1997**, *70*, 396.
(24) Piraux, L.; George, J. M.; Despres, J. F.; Leroy, C.; Ferain, E.; Legras, R.; Ounadjela, K.; Fert, A. *Appl. Phys. Lett.* **1994**, *65*, 2484.
(25) Li, Y.; Fan, Z. Y.; Lu, J. G.; Chang, R. P. H. *Chem. Mater.* **2004**, *16*, 2512.

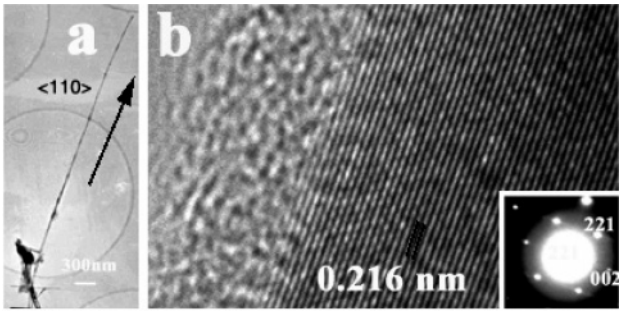

Figure 3. (a) A typical low-magnification TEM image of the Fe_3B nanowires. (b) The HR-TEM image and the corresponding SAED pattern (the inset) taken from part of a Fe_3B nanowire.

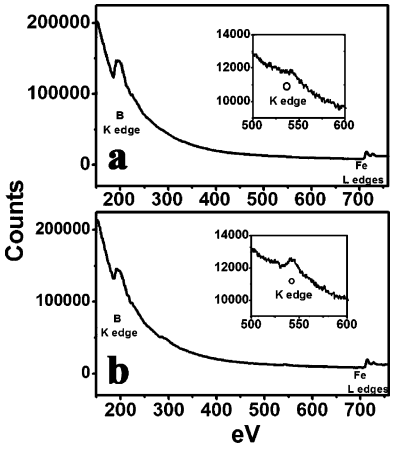

Figure 4. (a) An EELS (in STEM mode) spectrum taken from the center of a Fe_3B nanowire. (b) An EELS (in STEM mode) spectrum taken from the edge of the same nanowire.

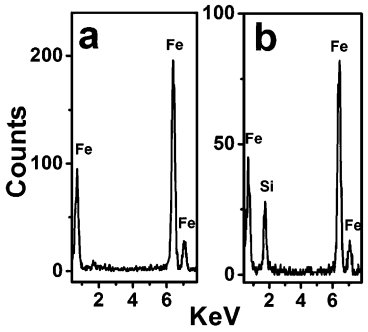

Figure 5. (a) An XEDS (in STEM mode) spectrum taken from the center of a Fe_3B nanowire. (b) An XEDS (in STEM mode) spectrum taken from the edge of the same nanowire.

is used, the particles with nanowires form all over the surface, with a relatively higher density on the scratches of the Si substrate.

The crystal structure and chemical composition of the nanowires and the particles formed when the temperature of the FeI_2 sublimator was kept in the range of 430−470 °C were studied by XRD, TEM, SAED, EELS, and XEDS. High-resolution TEM (HR-TEM), SAED, EELS, and XEDS (in STEM mode) studies (see Figures 3−5) on an individual nanowire indicate that the nanowires have the same crystal structure and element distribution of the single-crystal tetragonal Fe_3B nanowires produced on Pt/Pd-coated sapphire substrates.[17] The SAED pattern in Figure 3b can be indexed as a tetragonal Fe_3B phase (JCPDS 39-1316) with lattice constants of a = 8.6736 Å and c = 4.3128 Å recorded along the [$\bar{1}$10] zone axis.

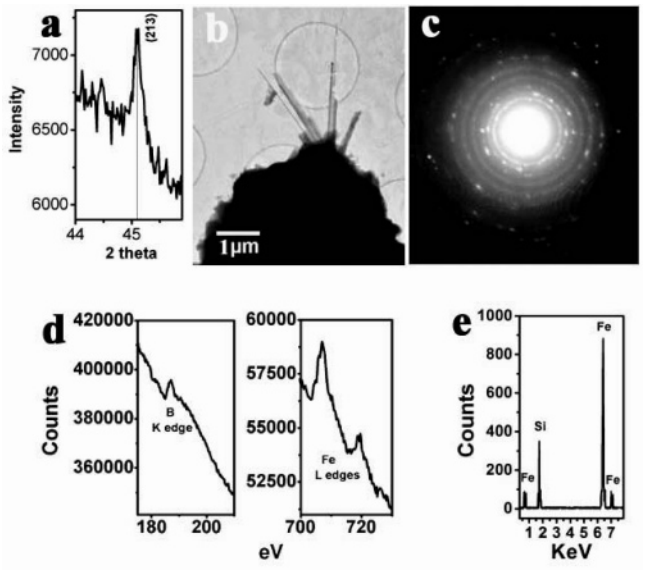

Figure 6. (a) An XRD pattern taken from the structures formed on a Si substrate at 800 °C with 20 sccm Ar gas carried FeI_2 vapor (FeI_2 sublimator temperature = 455 °C), 10 sccm Ar gas carried BI_3 vapor (BI_3 sublimator temperature = 31 °C), and 200 sccm diluting Ar gas flowing for 2 h. (b−e) A typical TEM image, a SAED pattern from part of a particle, an EELS spectrum taken from the edge of a particle, and an XEDS spectrum from part of a particle, respectively. The diffraction rings in the SAED pattern (from center to edge) can be indexed as the (202), (114), (204), (007), (008), and (500) peaks of a tetragonal Fe_5SiB_2 phase.

The HR-TEM image (see Figure 3b) clearly displays the 0.216 nm d spacing of the (002) planes. The axis of the nanowires is usually along the <110> direction, and there is a thin (2−5 nm) amorphous iron borate layer on the surface of each nanowire, which is also the same as the Fe_3B nanowires grown on Pt/Pd-coated sapphire substrates.[17] To explore the chemical composition and the crystal structure of the microscale particles, from which the Fe_3B nanowires grow, an XRD scan was performed on a sample made on a Si substrate. The result is shown in Figure 6a. The same sample was also studied by TEM, SAED, EELS, and XEDS. Figure 6a suggests that there is a small peak at 2θ = 45.1, which can be indexed as the (213) peak of a tetragonal Fe_5SiB_2 phase (JCPDS 19-0627). Figure 6b−e shows a typical TEM image, a SAED pattern from part of a particle, an EELS spectrum taken from the edge of a particle, and an XEDS spectrum from part of a particle, respectively. Figure 6d and e indicates that the particles contain boron, iron, and silicon. The SAED pattern in Figure 6c suggests that the particles are polycrystals. All the diffraction rings in the SAED pattern can be indexed as a tetragonal Fe_5SiB_2 phase (JCPDS 19-0627).

Growth Process of Fe_3B Nanowires. To understand the growth process of Fe_3B nanowires produced on bare SiO_2 on Si or Si substrates, time evolution of the Fe_3B nanowires synthesized on bare SiO_2 on Si substrates was studied. Figure 7a−d shows SEM images of the samples whose growth times are 5 min, 15 min, 1 h, and 2 h, respectively. The other growth parameters of the four samples are the same. There is nothing formed on the surface of the sample, for a growth time of 5 min. This suggests that there might be an incubation time for the growth of Fe_3B nanowires on bare SiO_2 on Si substrates. Figure 7b shows that, when the growth time is 15 min, there are some amorphous shaped particles with an average size of 5 μm on the scratches of the surface. As the reaction time is

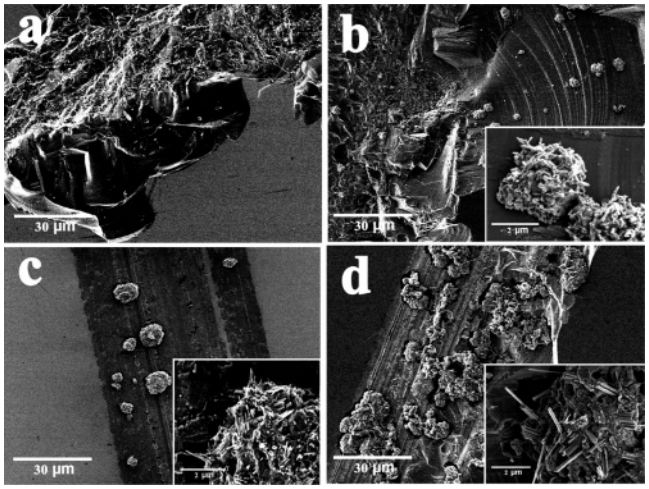

Figure 7. (a−d) SEM images of the samples whose growth times are 5 min, 15 min, 1 h, and 2 h, respectively. The other growth conditions of the four samples are the same: 800 °C growth temperature, 31 °C BI_3 sublimator temperature, 455 °C FeI_2 sublimator temperature, 200 sccm diluting Ar flow, 10 sccm carrier Ar with BI_3 flow, and 20 sccm carrier Ar with FeI_2 flow.

extended to 1 h, the particles become larger and some short nanowires grow out of the particles (see Figure 7c). Figure 7d indicates that longer nanowires are synthesized when the reaction time is increased to 2 h. As presented above, if no catalyst is employed, single-crystal Fe_3B nanowires grow out of polycrystalline Fe_5SiB_2 particles, which form around the scratches of SiO_2 on Si substrates or the surface of Si substrates. They cannot be produced on bare sapphire or bare fused silica substrates. This implies that the precursor vapor reacts with Si substrates to form Fe_5SiB_2 ($5FeI_2 + 2BI_3 + Si \rightarrow Fe_5SiB_2 + 8I_2$). For SiO_2 on Si substrates, Fe_5SiB_2 particles usually form on the scratches because the SiO_2 layer has been removed there. If Si substrates are used, Fe_5SiB_2 particles will form all over the surface. The scratches of the Si substrates have a higher yield of particles due to their lower nucleation barrier.

One-dimensional (1D) nanostructures grown from vapor-phase precursors are usually synthesized either by a vapor−liquid−solid (VLS) method or a vapor−solid (VS) method.[26−28] The VLS mechanism is used to explain the growth of 1D nanostructures with catalysts. A liquid agent is needed for the VLS growth mechanism, while the VS mechanism is used to explain the growth of 1D nanostructures from direct condensation of the precursor vapor. A low supersaturation is required for the growth of 1D structures. One-dimensional structures form due to anisotropic crystal growth or the existence of dislocations or defects. The B−Fe−Si ternary phase diagrams[29,30] show that there is no liquid solution involved in the B−Fe−Si system until 1100 °C. So the VLS mechanism does not apply to the growth of Fe_3B nanowires. At 800 C, Fe_5SiB_2[31,32] is a solid with a tetragonal structure. The lattice constant a of a tetragonal Fe_5SiB_2 ($a = 5.52$ Å) is 5/8 of the lattice parameter a of a tetragonal Fe_3B ($a = 8.69$ Å). So there is a lattice match between a tetragonal Fe_5SiB_2 phase and a tetragonal Fe_3B phase, and the surface of Fe_5SiB_2 particles can incorporate Fe_3B molecules efficiently.

On the basis of the results, we propose the growth process of Fe_3B nanowires as follows. Once FeI_2 vapor and BI_3 vapor are introduced, amorphous shaped Fe_5SiB_2 particles form first due to the reaction between the precursor vapor and the Si substrate. Both FeI_2 and BI_3 decompose at the growth temperature of 800 °C: $FeI_2 \rightarrow Fe + I_2$[33] (higher than 498 °C), $2BI_3 \rightarrow 2B + 3I_2$[34] (800 − 1000 °C). FeI_3 vapor and BI_3 vapor may react in the gas phase to form Fe_3B vapor[17] ($2FeI_2 + 6BI_3 \rightarrow 2FeB_3 + 11I_2$). The supersaturation of the chemical vapor is low, and the surface of the Fe_5SiB_2 particles may provide preferential sites for the adsorption of Fe_3B vapor, Fe vapor, and B vapor. The adsorbent Fe and B molecules may also react to form Fe_3B molecules on the surface of Fe_5SiB_2 particles. The Fe_3B molecules then nucleate and grow into Fe_3B nanowires due to the preferential growth along the <110> direction. As discussed above, the growth mechanism of Fe_3B nanowires can be considered as a VS-type process with the surface of Fe_5SiB_2 particles serving as the adsorption and nucleation sites.

Synthesis and Characterization of Fe_5Si_2B Nanowires. When the temperature of the FeI_2 sublimator was increased to 540−570 °C, bunches of nanowires formed on top of the triangle shaped particles. Similar to the Fe_3B nanowires, these nanowires with particles were produced around the scratches of SiO_2 on Si substrates or on the surface of Si substrates, as indicated by the SEM images shown in Figure 8.

The nanowires shown in Figure 8 have the same crystal structure and chemical composition. Figure 9a exhibits a typical low-magnification TEM image of the nanowires. A high-resolution TEM (HR-TEM) image taken from part of a nanowire and the corresponding SAED pattern is presented in Figure 9b. Both the SAED pattern and the HR-TEM image suggest that the nanowires are single crystals. The SAED pattern can be indexed as a tetragonal Fe_5Si_2B phase[29,31] (JCPDS 19-0626, $a = 8.80$ Å, $c = 4.32$ Å), recorded close to the $[\bar{1}11]$ zone axis. The HR-TEM image shows the 0.311 nm d spacing of the (220) planes. The axis of the nanowires is usually along the <110> direction. Figure 9b also displays a 2 nm thick amorphous layer on the surface of each nanowire. Element distribution in the nanowires was studied using EELS and XEDS in scanning transmission electron microscopy (STEM, 1 nm probe size) mode. Figure 10a and b illustrates typical EELS spectra taken from the center and the edge of a nanowire, respectively. They both display the characterization boron K edge, oxygen K edge, and iron L edges. The oxygen K edge in Figure 10b is more apparent than that in Figure 10a, which indicates that the amorphous layer on the surface of each nanowire is an oxide layer. Typical XEDS spectra taken from the center and the edge of a nanowire are exhibited in Figure 11a and b, respectively. Figure 11 suggests that the nanowires also contain Si. Compared to the center of a nanowire, the edge of a nanowire has more Si. From the HR-TEM, SAED, EELS, and XEDS study

(26) Levitt, A. P. *Whisker Technology*; Wiley-Interscience: New York, 1970.
(27) Wu, Y. Y.; Yang, P. D. *J. Am. Chem. Soc.* **2001**, *123*, 3165.
(28) Law, M.; Goldberger, J.; Yang, P. D. *Annu. Rev. Mater. Res.* **2004**, *34*, 83.
(29) Villars, P.; Prince, A.; Okamoto, H. *Handbook of ternary alloy phase diagrams*; ASM International: Materials Park, OH, 1995.
(30) Efimov, Y. V.; Mukhin, G. G.; Lazarev, E. M.; Korotkov, N. A.; Ryabtsev, L. A.; Dmitriev, V. N.; Frolova, T. M. *Izv. Akad. Nauk SSSR Metall.* **1986**, *4*, 167.
(31) Chaban, N. F.; Kuz'ma, Y. B. *Izv. Akad. Nauk SSSR Neorg. Mater.* **1970**, *6*, 1007.
(32) Aronsson, B.; Engstrom, I. *Acta Chem. Scand.* **1960**, *14*, 1403.
(33) Zaugg, W. E.; Gregory, N. W. *J. Phys. Chem.* **1966**, *70*, 486.
(34) Holleman, A. F.; Wiberg, E. *Inorganic Chemistry*; Academic Press: New York, 2001.

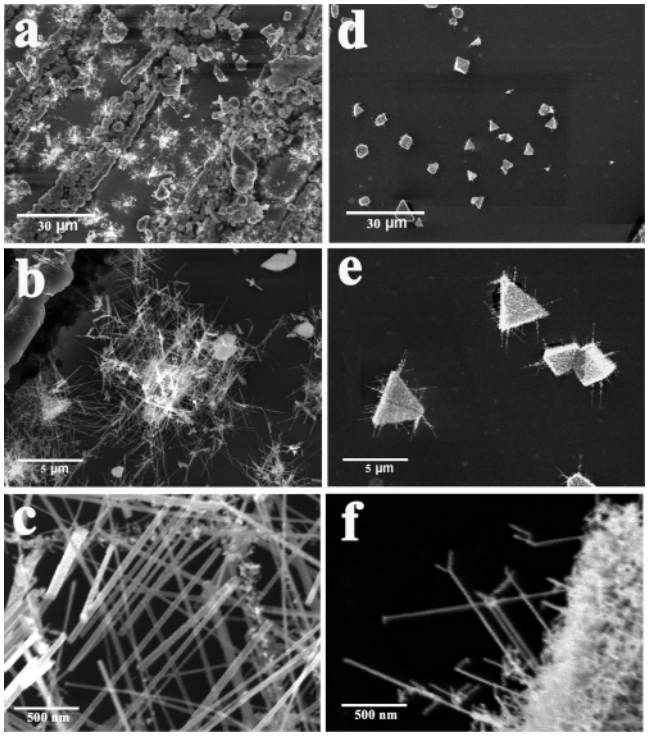

Figure 8. (a−c) SEM images of the nanowires formed on a SiO_2 on Si substrate at 800 °C with 10 sccm Ar gas carried FeI_2 vapor (FeI_2 sublimator temperature = 560 °C), 10 sccm Ar gas carried BI_3 vapor (BI_3 sublimator temperature = 31 °C), and 200 sccm diluting Ar gas flowing for 0.5 h. (d−f) SEM images of the nanowires synthesized on a Si substrate after heating at 800 °C under 10 sccm Ar gas carried FeI_2 vapor (FeI_2 sublimator temperature = 550 °C), 10 sccm Ar gas carried BI_3 vapor (BI_3 sublimator temperature = 31 °C), and 200 sccm diluting Ar gas flow for 1 h.

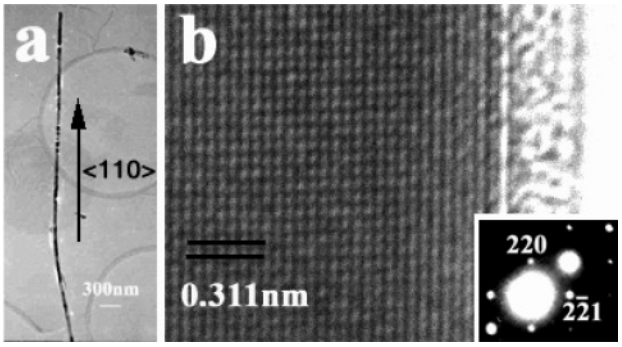

Figure 9. (a) A typical low-magnification TEM image of the Fe_5Si_2B nanowires. (b) The HR-TEM image and the corresponding SAED pattern (the inset) taken from part of a Fe_5Si_2B nanowire.

presented above, the as grown nanowires are single-crystal Fe_5Si_2B covered with thin amorphous iron silicon boron oxide layers.

Figure 8a also suggests that there are some particles formed on the scratches, which do not have nanowires grown on them. To explore the crystal phases produced, XRD was performed on the sample, whose SEM images are shown in Figure 8a−c. All the peaks in the XRD pattern (shown in Figure 12a) can be indexed as either an orthorhombic $FeSi_2$ phase (JCPDS 71-0642) or a cubic FeSi phase (JCPDS 86-0793). TEM, SAED, EELS, and XEDS studies indicate that the particles which do not have nanowires grown are $FeSi_2$ single crystals, while the triangle shaped particles, which have nanowires grown are FeSi single crystals. EELS from both kinds of particles suggests that they do not contain boron. Figure 12c−e shows a TEM image, the

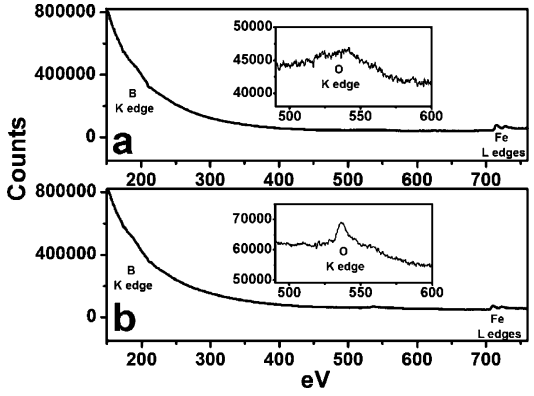

Figure 10. (a) An EELS spectrum (in STEM mode) taken from the center of a Fe_5Si_2B nanowire. (b) An EELS spectrum (in STEM mode) taken from the edge of the same nanowire.

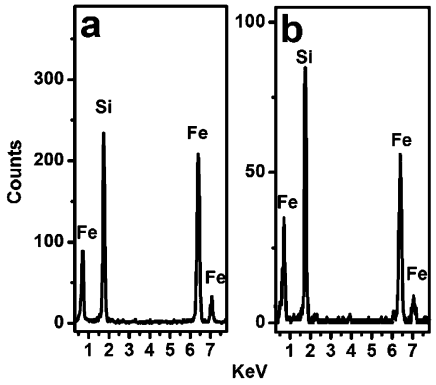

Figure 11. (a) An XEDS spectrum (in STEM mode) taken from the center of a Fe_5Si_2B nanowire. (b) An XEDS spectrum (in STEM mode) taken from the edge of the same nanowire.

corresponding SAED pattern, and an XEDS spectrum from the $FeSi_2$ particles, respectively. The SAED pattern in Figure 12d can be indexed as an orthorhombic $FeSi_2$ phase (JCPDS 71-0642) recorded close to the $[\bar{3}\bar{2}2]$ zone axis. Figure 12f−h presents a TEM image, the corresponding SAED pattern, and an XEDS spectrum from the triangle shaped FeSi particles, respectively. The SAED pattern in Figure 12g may be indexed as a cubic FeSi phase (JCPDS 86-0793) recorded along the [001] zone axis.

Growth Process of Fe_5Si_2B Nanowires. Time evolution of the Fe_5Si_2B nanowires was studied by making a series of samples, which have the same growth conditions except the growth time. Their SEM images are shown in Figure 13. Figure 13a presents an SEM image from the sample, whose growth time is 15 min. It clearly shows that the nanowires grow from the triangle shaped particle. The inset in Figure 13a indicates that the nanowires tend to nucleate first on the two edges of the triangle shaped particles. The angle between the two edges is about 60°. The nanowires grow longer if the growth time is increased, as shown in Figure 13b,c. When the growth time is increased to 1 h, the triangle shaped particles beneath the nanowires are barely visible from the SEM image shown in Figure 13c. The sample, whose SEM image is shown in Figure 13a, was studied by TEM, SAED, XEDS, and EELS to further explore the growth process of the Fe_5Si_2B nanowires. Figure 14a displays a TEM image of a triangle shaped FeSi particle. It shows that a nanowire grows from the layer attached to the particle. An SAED pattern taken from the particle is shown in

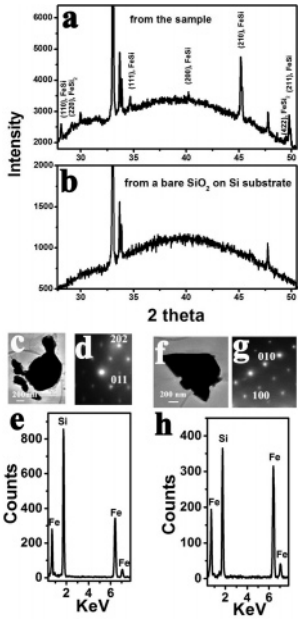

Figure 12. (a) An XRD pattern from a sample (its SEM images are shown in Figure 8a−c) formed on a SiO_2 on Si substrate at 800 °C with 10 sccm Ar gas carried FeI_2 vapor (FeI_2 sublimator temperature = 560 °C), 10 sccm Ar gas carried BI_3 vapor (BI_3 sublimator temperature = 31 °C), and 200 sccm diluting Ar gas flowing for 0.5 h. (b) An XRD pattern from a bare SiO_2 on Si substrate. (c−e) A typical TEM image, the corresponding SAED pattern, and an XEDS spectrum taken from the $FeSi_2$ particles on the scratches. (f−h) A typical TEM image, the corresponding SAED pattern, and an XEDS spectrum taken from the triangle shaped FeSi particles around the scratches.

Figure 14b. It can be indexed as a cubic FeSi phase (JCPDS 86-0793) recorded along the $[0\bar{1}1]$ zone axis. According to the SAED pattern, the three planes, which form the three edges of the triangle shaped particle, can be considered as the $(\bar{1}\bar{1}\bar{1})$, $(\bar{1}11)$, and (100) planes (see Figure 14a). EELS and XEDS spectra taken from the particle indicate that it contains only Fe and Si. The nanowire and the layer attached to the triangle shaped particle have the same crystal structure and chemical composition. An SAED pattern taken from the layer is shown in Figure 14c, which may be indexed as a tetragonal Fe_5Si_2B phase recorded close to the $[2\bar{2}\bar{2}]$ zone axis. EELS and XEDS spectra taken from the layer indicate that it contains boron, iron, and silicon. The inset in Figure 14a shows schematically how the SAED pattern from the particle is related to the SAED pattern from the Fe_5Si_2B layer. The *d* spacing of the $(\bar{1}11)$ planes of a cubic FeSi phase is (JCPDS 86-0793) 2.59 Å, which is very close to the *d* spacing of the $(2\bar{2}1)$ planes of a tetragonal Fe_5Si_2B phase (2.52 Å, JCPDS 19-0626). The TEM image and the two SAED patterns suggest that the Fe_5Si_2B layer epitaxially grows from the $(\bar{1}\bar{1}\bar{1})$ plane of the triangle shaped particle. A $(\bar{1}\bar{1}\bar{1})$ plane and a $(\bar{1}11)$ plane are equivalent to a (111) plane for a cubic phase. The angel between the two planes is 60°. Combined with the SEM result shown in Figure 13a, it is apparent that the Fe_5Si_2B layers and nanowires tend to nucleate first on the {111} planes of FeSi triangle shaped particles.

On the basis of the results presented above, we propose here the growth process of Fe_5Si_2B nanowires as follows. When FeI_2 and BI_3 vapor are introduced, triangle shaped FeSi particles form due to the reaction between FeI_2 vapor and the Si substrate ($FeI_2 + Si \rightarrow FeSi + I_2$). FeI_2 vapor and BI_3 vapor may react with the Si substrate to form Fe_5Si_2B vapor ($5FeI_2 + 2BI_3 + 2Si \rightarrow Fe_5Si_2B + 8I_2$). Fe_5Si_2B vapor is then preferentially adsorbed on the {111} planes of triangle shaped FeSi particles. The adsorbent Fe_5Si_2B molecules epitaxially grow into Fe_5Si_2B layers from the surface of FeSi particles. Fe_5Si_2B nanowires grow out of the Fe_5Si_2B layers due to preferred growth along the <110> direction. Analogous to the Fe_3B nanowires, the growth mechanism of Fe_5Si_2B nanowires is a VS-type process with {111} planes of FeSi particles as the adsorption and nucleation sites.

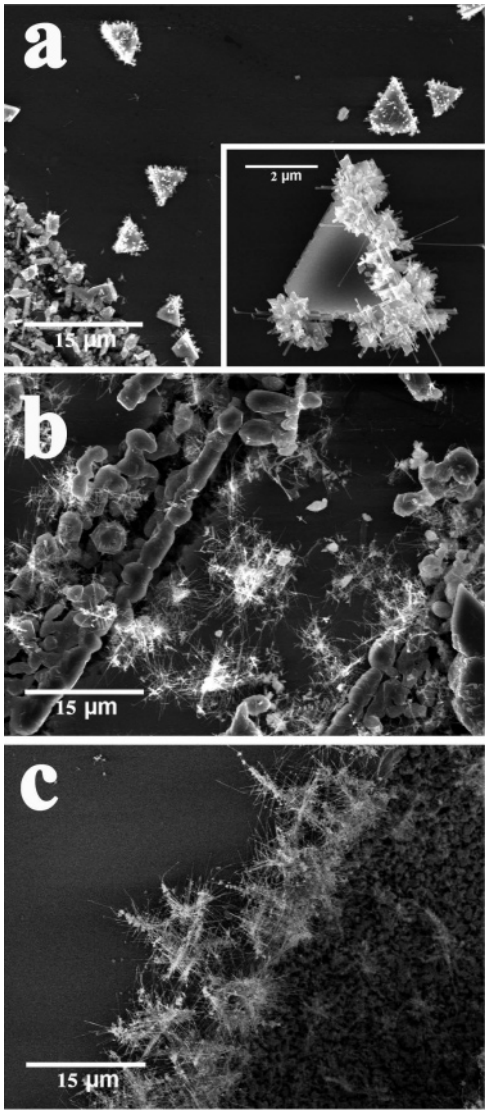

Figure 13. (a−c) SEM image of the sample whose growth time is 15 min, 0.5 h, and 1 h, respectively. The other growth conditions of the three samples are the same: substrate temperature = 800 °C, diluting Ar flow = 200 sccm, carrier Ar with FeI_2 (FeI_2 sublimator temperature = 560 °C) flow = 10 sccm, carrier Ar with BI_3 (BI_3 sublimator temperature = 31 °C) flow = 10 sccm.

Conclusions

A CVD method was developed to grow both Fe_3B nanowires and Fe_5Si_2B nanowires without introducing any catalysts. SiO_2 on Si or Si wafers were used as substrates. BI_3 and FeI_2 were employed as precursors. Various kinds of Fe−Si−B and Fe−Si structures were synthesized by modifying the ratio of FeI_2 vapor to BI_3 vapor. The amount of FeI_2 or BI_3 vapor introduced in the chamber is determined by its vapor pressure and the flow

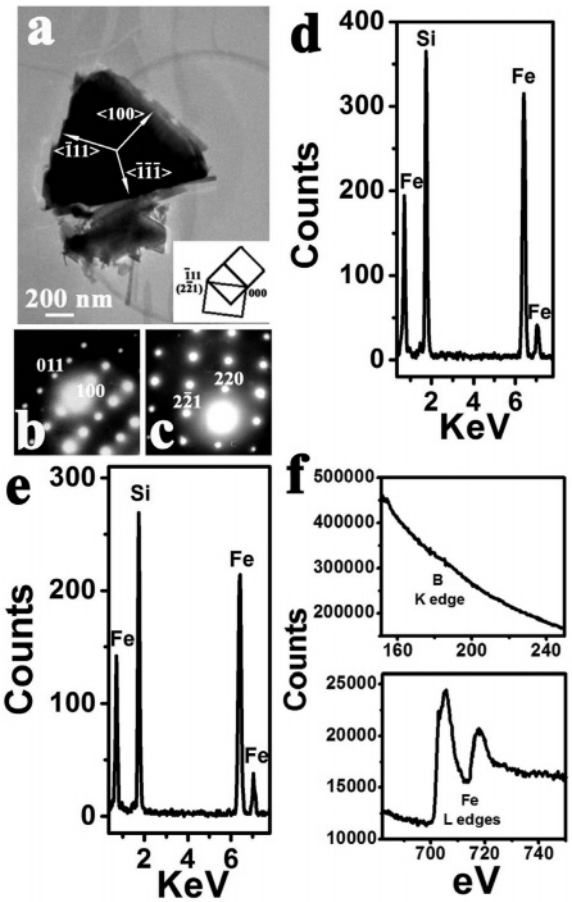

Figure 14. (a) A TEM image of the FeSi triangle shaped particles (the SEM images of the sample are shown in Figure 13(a)). (b) An SAED pattern taken from the FeSi particle. (c) A typical SAED pattern taken from the Fe_5Si_2B layer attached to the FeSi particle or the nanowire. (d) An XEDS spectrum taken from the FeSi particle. (e and f) A typical XEDS and an EELS spectrum from the Fe_5Si_2B layer, respectively.

rate of its carrier gas. The vapor pressure can be controlled by the temperature of the sublimator. We kept the flow rate of each carrier gas and the temperature of BI_3 sublimator unchanged. Adjusting FeI_2 sublimator temperature actually modifies the ratio of FeI_2 vapor to BI_3 vapor. The higher the FeI_2 sublimator temperature, the higher the ratio of FeI_2 vapor to BI_3 vapor. If the FeI_2 sublimator temperature was kept in the range of 430−470 °C, single-crystal Fe_3B nanowires formed. As the FeI_2 sublimator temperature was adjusted in the range of 540−570 °C, single-crystal Fe_5Si_2B nanowires were produced. The quantitative amount of FeI_2 vapor to BI_3 vapor ratio at different FeI_2 sublimator temperature was not measured. The CVD apparatus will be modified to insert sensors for the measurement in the future.

Fe_3B and Fe_5Si_2B nanowires grow due to the following two factors: (1) the correct ratio of FeI_2 vapor to BI_3 vapor, which allows the Fe_3B or Fe_5Si_2B phase to form; (2) the formation of Fe_5SiB_2 or FeSi particles, which provide preferential sites for the adsorption and nucleation of Fe_3B or Fe_5Si_2B molecules.

Room temperature magnetic force microscopy (MFM) investigations on the Fe_3B nanowires suggest that they are ferromagnetic nanowires with a single domain configuration.[17] Fe_5Si_2B nanowires were dispersed in isopropyl alcohol by sonication and then deposited onto a SiO_2 on Si substrate for MFM studies. However, there are always large micron size particles distributed around the nanowires. Decent MFM images cannot be obtained due to the rough surface. A new sample preparation method needs to be developed in the future for MFM studies of Fe_5Si_2B nanowires.

Acknowledgment. This work was supported by the B NIRT NSF grant (29212S/WU-HT-02-33/NSF-EEC-0210120). We appreciate helpful discussion with Dr. D. Bruce Buchholz (on CVD system). We acknowledge the use of MRSEC facilities: EPIC, NIFTI, J.B. Cohen XRD Facilities at Northwestern University (NSF-DMR 0520513).

Supporting Information Available: Morphology, crystal structure, and chemical composition of other structures in Table 1. This material is available free of charge via the Internet at http://pubs.acs.org.

JA0610378